

Hyperacuity: Application to visual stabilization

Colonnier F.¹, Manecy A.^{1,2}, Juston R.¹, Viollet S.¹

¹*Aix Marseille Université, CNRS, ISM UMR 7287, 13288, Marseille, France*
stephane.viollet@univ-amu.fr

²*ONERA, DCSD/CT, The French Aerospace Lab, 31055 Toulouse, France*

Abstract

Here we present the active CurvACE and its visual processing algorithm using sinusoidal vibration. The specific architecture and active tremor of the eye enhance its spacial resolution leading to a great positioning of the sensor relative to the environment. Therefore, in the present paper, we used a fully autonomous sighted twin-rotor robot with two degrees of freedom named HyperRob, which was equipped with the active CurvACE. Thanks to its roll stabilization, HyperRob is able to sense linear displacements relative to the visual environment with a field of view composed of only 8 by 5 ommatidia (40 pixels). The robot compensated efficiently for strong lateral disturbances and large displacements of the visual environment (a printed panel). Experimental results confirmed that our active compound eye was endowed with hyperacuity and it can be a suitable candidate for providing the micro aerial robotic platforms of the future with visual odometry.

1 Introduction

In this study, a miniature artificial compound eye (15mm in diameter) named CurvACE (Curved Artificial Compound Eye [1]) was endowed with hyperacuity. According to the definition proposed by G. Westheimer [2]: "Hyperacuity refers to sensory capabilities in which the visual sensor transcends the grain imposed by its anatomical structure". In the case of vision, it means that an eye is able to locate visual objects with a greater accuracy than the angular difference between two neighboring photoreceptors $\Delta\varphi$. To implement hyperacuity on an artificial compound eye, a periodic micro-scanning movement of only a few degrees was used to make the artificial compound eye locate contrasting objects with a 40-fold greater resolution than that imposed by the interommatidial angle. This approach was inspired by the retinal micro-movements observed in the eye of the blowfly *Calliphora* [3]. With such a sensor, it was possible to achieve with a high accuracy challenging robotic tasks like hovering and odometry [4].

2 Description of the Visual Sensor

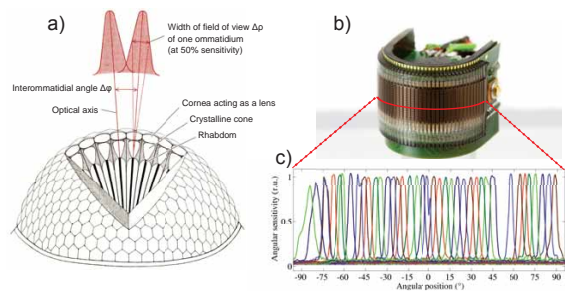


Figure 1: **(a)** Schematic view of a compound eye, showing the two main optical parameters of interest: the interommatidial angle $\Delta\varphi$, defined as the angle between optical axes of two adjacent ommatidia, and the acceptance angle $\Delta\rho$, defined as the angle at half width of the Gaussian shaped ASF. Adapted with permission from [5]. **(b)** CurvACE sensor and **(c)** the horizontal angular sensitivity functions (ASFs) measured for each artificial ommatidium along the equatorial row (red line). The mean value of the interommatidial angle $\Delta\varphi$ obtained in the middle row (red line) is $4.2^\circ \pm 1.17^\circ$ (SD) and that of the acceptance angle is $4.2^\circ \pm 0.56^\circ$ (SD).

In its active version, the CurvACE eye has been endowed with the following unexpected but useful properties:

- a low spatial resolution, which reduces the processing burden (figure 1)
- a blurred vision, which acts like an analog spatial low-pass filter (figure 1)
- visual micro-scanning movements generated by a tiny eccentric mechanism. (figure 2b)

Unlike the fly's retinal scanning movements, which result from the translation of the photoreceptors (see figure 2a) in the focal plane of each individual facet lens (for a review on the fly's retinal micro-movements see [6]), the eye tremor applied here to the active CurvACE by means of a micro-stepper motor with an eccentric shaft (figure 2b)

results in a periodic rotation of the whole artificial compound eye.

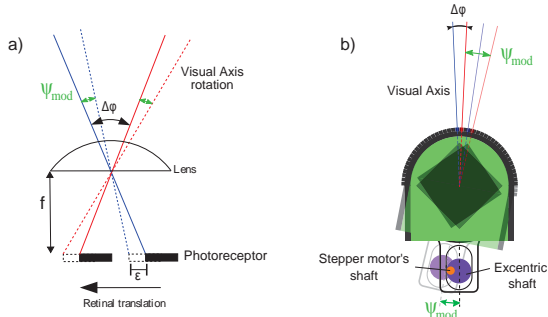


Figure 2: Optical axis rotation resulting from (a) a micro-displacement ε of the pixels placed behind a fixed lens (e.g., in the case of a compound eye of the fly) or (b) a rotation of the whole sensor (e.g., in the case of the active CurvACE sensor). The micro-scanning of active CurvACE is subjected to active periodic rotational movements ψ_{mod} generated by a miniature eccentric mechanism.

2.1 Visual Algorithm

Based on the previous knowledge designing 2-pixel vibrating sensors ([7], [8], [9], [10]), it has been shown that it is possible to locate feature with a great accuracy. Moreover, Juston *et al.* [11] prove that it is possible to discriminate an edge from a bar and to give the position of the defined feature. However, this study still involved only 2-pixels.

With active CurvACE, it is now possible to use a large Region Of Interest (ROI) of several pixels and duplicate the Local Processing Unit previously developed. Figure 3 depicts the fusion algorithm which leads to position and speed measurement. This novel sensory fusion algorithm which is based on the selection of the 10 highest contrasts, enables the active eye (2D-FOV: 32° by 20°) to assess its displacement with respect to a textured environments.

3 Robotic Application

3.1 Objectives

The objective was here to endow a visually controlled robot, named HyperRob, with the capability to:

- stay at a desired position (reference position) with respect to the visual environment (a textured panel, see figure 4)
- return to the reference position even in the presence of perturbation applied to the robot (lateral disturbance) or the textured panel over which the robot is flying.

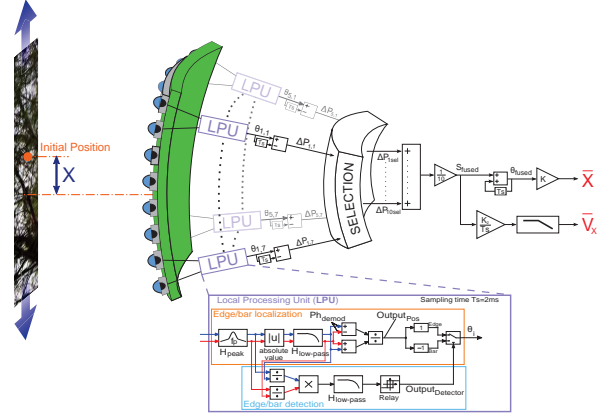


Figure 3: Description of the sensory fusion algorithm to assess the robot's speed \bar{V}_x as well as its position \bar{X} resulting here from a translation of the textured panel with respect to the arbitrary reference position (i.e. the initial position if not resetting during the flight). The 40 artificial ommatidia (8×5) of the active CurvACE were processed by the 35 (7×5) Local Processing Units (LPUs). Then, a mean of 10 selected $\Delta P_{i,j}$ is used to compute the linear speed and position.

3.2 Experimental setup

HyperRob equipped with active CurvACE is a twin-rotor robot tethered at the tip of a rotating arm. The robot was free to rotate around its roll axis and could therefore make the arm rotate around its vertical axis (the azimuth). The robot travelled along a circular path with a radius of curvature equal to the length of the arm (1m). Figure 4 shows the robot with active CurvACE placed on the experimental testbench.

In the following section, the experiments shows that the robot is able to stay at its initial position thanks to the vibrating active CurvACE estimating its linear speed and position, assuming that its gaze is stabilized.

3.3 Experimental results

3.3.1 Lateral disturbance rejection above a horizontal textured panel

Lateral disturbances were applied by pushing the arm in both directions simulating gusts of wind. In figure 5, it can be seen that all the lateral disturbances were completely rejected within about 5 seconds, including even those as large as 40cm. Figure 5b and 5c show that the robot was always able to return to its initial position. With its active eye, the robot can compensate for lateral disturbance as large as 359mm applied to its reference position with a maximum error of only 25mm, i.e. 3% of the flown distance.

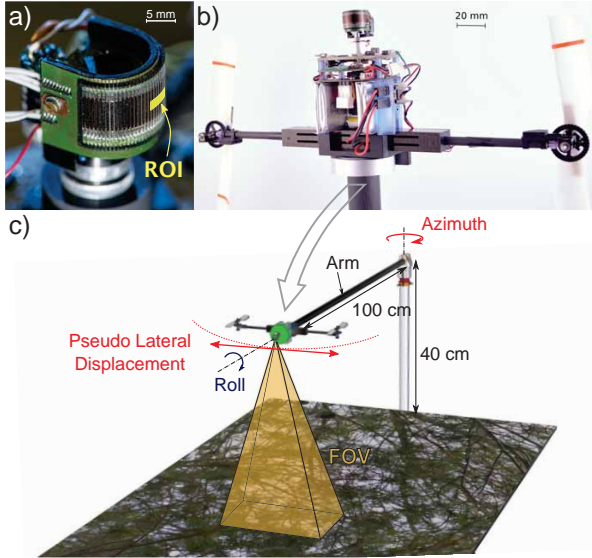


Figure 4: Experimental setup of the robot HyperRob

a) Active CurvACE with a region of interest (inset) composed of only 40 artificial ommatidia (8×5), each photosensor is composed of one pixel and one lens. The field of view (FOV) covers about 33.6° by 20.2° . (Picture provided by courtesy of P. Psaila)

b) The robot HyperRob and its active CurvACE sensor.

c) The complete setup consisted of a twin-propeller robot attached to the tip of a rotating arm. The robot was free to rotate around its roll axis. Arm rotations around the azimuth were perceived by the robot as lateral displacements.

3.3.2 Stabilization relative to a moving ground

In this experiment, the panel was moved manually and the robot's reference position setpoint X^* was kept at zero. The robot faithfully followed the movements imposed on the panel. The few oscillations which occurred were mainly due to the robot's dynamics rather than to visual measurement errors. Each of the panel's movements was clearly detected, as shown in figure 6, although a proportional error in the measurements was sometimes observed, as explained above.

4 Conclusion

In this paper, we describe a vibrating small-scale cylindrical curved compound eye, named active CurvACE. The active process referred to here means that miniature periodic movements have been added in order to improve CurvACE's spatial resolution in terms of the localization of visual objects encountered in the surroundings. Hyperacuity was achieved here by 35 Local Processing Units ap-

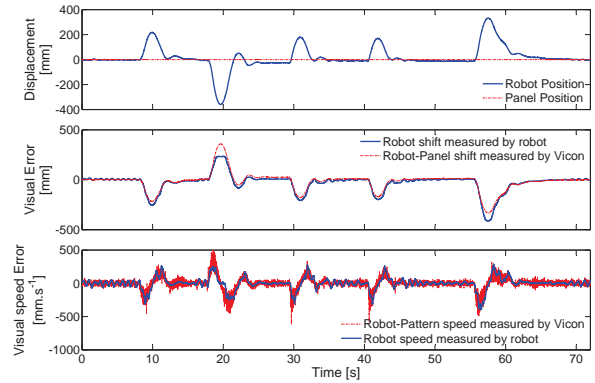


Figure 5: Lateral disturbance rejection over a naturally textured Panel

a) Robot's position (in blue) superimposed on the panel's position (in red), both measured by the VICON system.

b) The visual errors measured by the robot (red) and the VICON (blue) were very similar. With large disturbances, small errors occurred in the visual estimation of the robot's position without noticeably affecting the robot's capability to return automatically to its starting position.

c) Ground-truth measurement of the robot speed error (red curve) and the visual speed error (blue curve) measured by the robot thanks to active CurvACE.

plying the same local visual processing algorithm across a ROI of active CurvACE consisting of 8×5 artificial ommatidia.

All the solutions adopted in this study in terms of practical hardware and computational resources are perfectly compatible with the stringent specifications applying to low-power, small sized, low-cost micro-aerial vehicles (MAVs). Indeed, thanks to active CurvACE, we achieved very accurate hovering flight with few computational resources (only two 16-bit micro controller and few pixels (only 8×5). However, the 1D visual scanning presented here is not enough to enable free flight which would require a novel 2D scanning system or another eye.

ACKNOWLEDGMENT

The authors would like to thank Marc Boyron and Julien Dipéri for the robot and the test bench realization; Nicolas Franceschini for helping in the design of the robot, Franck Ruffier for the fruitful discussions. We also acknowledge the financial support of the Future and Emerging Technologies (FET) program within the Seventh Framework Programme for Research of the European Commission, under FET-Open Grant 237940. This work was supported by CNRS, Aix-Marseille University, Provence-Alpes-Cote d'Azur region and the French National Research Agency (ANR) with the IRIS

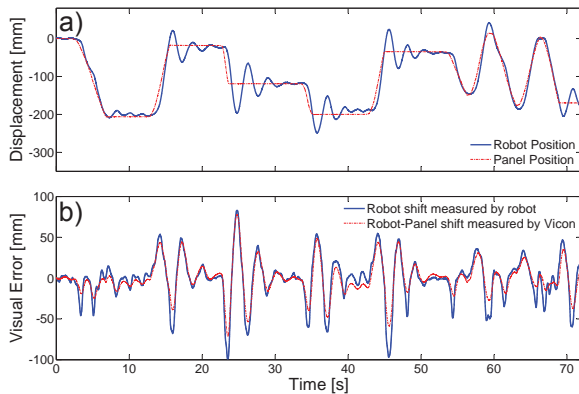


Figure 6: Tracking a naturally textured Panel When the textured panel was moved manually below the robot, HyperRob automatically followed the movement imposed by the panel.

a) Tracking of the panel by the robot. The red line corresponds to the panel's position and the blue line to the robot's position, both measured by the VICON system.

b) Comparison between the position measurement error given by the visual system (in blue) and the ground truth data (in red) given by the VICON system. The results show that the robot tracked the moving panel accurately with a maximal position estimation error of 39mm for a panel translation of 150mm .

and Equipex/Robotex projects (IRIS project under ANR grants' number ANR-12-INSE-0009).

References

References

- [1] D. Floreano, R. Pericet-Camara, S. Viollet, F. Ruffier, A. Brckner, R. Leitel, W. Buss, M. Menouni, F. Expert, R. Juston, M.K. Dobrzynski, G. L'Eplattenier, F. Recktenwald, H.A. Mallot, and N. Franceschini. Miniature curved artificial compound eyes. *Proceedings of the National Academy of Sciences of the United States of America*, 110(23):9267–9272, June 2013.
- [2] G. Westheimer. Hyperacuity. *Encyclopedia of Neuroscience*, 5:45–50, 2009.
- [3] N. Franceschini and R. Chagneux. Repetitive scanning in the fly compound eye. In *Göttingen Neurobiology Report*, volume 2. Thieme, 1997.
- [4] F. Colonnier, A. Manecy, R. Juston, H. Mallot, R. Leitel, D. Floreano, and S. Viollet. A small-scale hyperacute compound eye featuring active eye tremor: application to visual stabilization, target tracking, and short-range odometry. *Bioinspiration & biomimetics*, 10(2):026002, 2015.
- [5] G. A. Horridge. The compound eye of insects. *Scientific American*, 237:108–120, 1977.
- [6] S. Viollet. Vibrating makes for better seeing: from the fly's micro eye movements to hyperacute visual sensors. *Frontiers in Bioengineering and Biotechnology*, 2(9), 2014.
- [7] S. Viollet and N. Franceschini. Biologically-inspired visual scanning sensor for stabilization and tracking. In *Intelligent Robots and Systems, 1999. IROS '99. Proceedings. 1999 IEEE/RSJ International Conference on*, volume 1, pages 204–209vol.1, 17-21 Oct. 1999.
- [8] L. Kerhuel, S. Viollet, and N. Franceschini. Steering by gazing: An efficient biomimetic control strategy for visually guided micro aerial vehicles. *Robotics, IEEE Transactions on*, 26(2):307–319, April 2010.
- [9] S. Viollet and N. Franceschini. A hyperacute optical position sensor based on biomimetic retinal micro-scanning. *Sensors and Actuators A: Physical*, 160(1-2):60 – 68, 2010.
- [10] L. Kerhuel, S. Viollet, and N. Franceschini. The vodka sensor: A bio-inspired hyperacute optical position sensing device. *Sensors Journal, IEEE*, 12(2):315–324, 2012.
- [11] R. Juston, L. Kerhuel, N. Franceschini, and S. Viollet. Hyperacute edge and bar detection in a bioinspired optical position sensing device. *Mechatronics, IEEE/ASME Transactions on*, 19(3):1025–1034, June 2014.